

→ Bio 463A: PLEASE READ SECTIONS
marked w/ *

Annu. Rev. Biophys. Biomol. Struct. 1992. 21:441-83
Copyright © 1992 by Annual Reviews Inc. All rights reserved

D. M. Engelman, Ed.

STRUCTURE AND MECHANISM OF ALKALINE PHOSPHATASE

Joseph E. Coleman

Department of Molecular Biophysics and Biochemistry, Yale University,
New Haven, Connecticut 06510

KEY WORDS: zinc enzymes, enzyme mechanisms (alkaline phosphatase), crystal
structure (alkaline phosphatase), ^{31}P NMR (alkaline phosphatase), ^{113}Cd NMR (alkaline phosphatase)

CONTENTS

INTRODUCTION	442
GENERAL STRUCTURE OF <i>E. COLI</i> ALKALINE PHOSPHATASE	443
SUMMARY OF SUBSTRATE SPECIFICITY AND KINETICS OF ALKALINE PHOSPHATASE	443
THE METALLOENZYME NATURE OF ALKALINE PHOSPHATASE	453
COORDINATION CHEMISTRY AT THE ACTIVE CENTER OF ALKALINE PHOSPHATASE	456
<i>Zn1(A) Coordination</i>	460
<i>Zn2(B) Coordination</i>	460
<i>Mg3(C) Coordination</i>	460
<i>Enzyme-Bound Phosphate in the E·P Intermediate</i>	461
<i>Enzyme-Bound Phosphate in the E-P Intermediate</i>	461
CHANGES IN ACTIVITY OF ALKALINE PHOSPHATASE ON SUBSTITUTING CADMIUM, COBALT, OR MANGANESE FOR THE NATIVE ZINC ION	463
CONCLUSIONS ON STRUCTURE AND MECHANISM OF ALKALINE PHOSPHATASE DERIVED FROM MULTINUCLEAR NMR	464
CORRELATION OF STRUCTURE AND MECHANISM	468
<i>Michaelis Complex with a Phosphate Monoester</i>	468
<i>The Phosphoseryl Intermediate</i>	469
<i>Hydrolysis of the Phosphoseryl Intermediate</i>	469
<i>Dissociation of the Product, Inorganic Phosphate, the Rate-Limiting Step</i>	470
<i>The Phosphotransferase Reaction</i>	471
SUMMARY OF THE MECHANISM OF ALKALINE PHOSPHATASE AS BASED ON SOLUTION DATA AND THE CRYSTAL STRUCTURE	473
SITE-DIRECTED MUTANTS OF <i>E. COLI</i> ALKALINE PHOSPHATASE	476
<i>Ser102 → Cys102, Ala102, Leu102</i>	477
<i>Arg166 → Lys166, Glu166, Ser166, Ala166</i>	477
<i>Lys328 → His328, Ala328</i>	478
SUMMARY	480

* INTRODUCTION

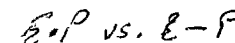
Alkaline phosphatase is often cited as the most frequently referenced enzyme (55). This fact relates more to the widespread use of alkaline phosphatase activity in human serum as an enzymatic signal for a variety of disease states involving particularly the liver and bone, than to a greater number of investigations directed at the molecular properties of the enzyme. The emergence in the literature of the enzyme alkaline phosphatase began around 1907 when Suzuki et al first suggested that phosphatases constituted a separate class of eukaryotic enzymes (70). By 1912, the enzyme we now know as alkaline phosphatase was defined by the work of Grosser & Husler (40) and von Euler (75), who showed that while it was present in a variety of tissues, the enzyme, which could hydrolyze glycerophosphate and fructose 1-6 diphosphate, was present in highest amount in intestinal mucosa. von Euler & Funke (76) used the word phosphatase for the first time in 1912. The enzyme from intestinal mucosa, particularly calf intestine, became the prototype for investigators exploring the properties of the enzyme itself.

Not until 1961 did Engstrom discover that the intestinal enzyme formed a phosphoseryl residue when incubated with phosphate esters at low pH (27, 28). The enzyme's catalysis of ^{18}O exchange into inorganic phosphate strongly supported the notion that the phosphoserine is a significant intermediate on the catalytic pathway (3, 65, 69). The demonstration that transfer of phosphate by the enzyme from an ester to a second alcohol leads to retention rather than inversion of configuration around the phosphorous (46) supported the conclusion derived from much previous evidence that the mechanism involves two sequential in-line nucleophilic attacks at phosphorous, the first by the hydroxyl of Ser102 on the incoming phosphomonoester and the second on the phosphoseryl intermediate by solvent water or an alcohol acceptor (32-34, 38).

In the late 1950s and early 1960s, investigators discovered that *Escherichia coli* possessed an alkaline phosphatase that was derepressible by phosphate starvation (21, 31, 42, 72). Its gene, *phoA*, was part of the *pho* regulon consisting of the group of genes in *E. coli* whose products are involved in phosphate transport and metabolism (4, 22, 38, 53) (for bibliography, see 22, 38). The *E. coli* enzyme had similar catalytic properties, similar pH-rate profile, and formed the same phosphoseryl intermediate as the intestinal enzyme (66, 67). The amino acid sequences of the mammalian enzymes, derived from their cDNA sequences, can be fit into the primary structure of the bacterial enzyme, with the proper adjustments for some insertions and deletions (47). With such adjustments, most of the critical active-site residues described below are conserved between the eukaryotic and bacterial enzymes.

In 1962, the *E. coli* alkaline phosphatase joined the class of zinc metallo-enzymes with the demonstration by Plocke et al (62) that the enzyme contained stoichiometric amounts of zinc, a finding also confirmed in later studies of the calf intestinal enzyme (30). These early studies showed that Zn(II) is required for activity, and many subsequent studies have confirmed this observation, including the demonstration that the metal is required for initial phosphate binding and thus for the formation of the phosphoseryl intermediate (3). The great stability over a wide range of pH of the metal-free apophosphoryl enzyme, which can be formed by removal of the metal ion from the Cd(II) enzyme, demonstrates that the metal ion is required for dephosphorylation of the phosphoseryl intermediate as well (18).

The most detailed information on the structure and function of the enzyme is available for the *E. coli* enzyme. This review is a synthesis of the solution data and the recently completed crystal structures of the *E. coli* alkaline phosphatase and its two phosphoenzyme intermediates at 2.0-Å and 2.5-Å resolution, respectively (48). The phosphoenzymes are (E·P) the noncovalent complex formed between inorganic phosphate and the enzyme, and (E-P) the covalent or phosphoseryl intermediate, formed by the phosphorylation of Ser102.

* GENERAL STRUCTURE OF *E. COLI* ALKALINE PHOSPHATASE

Alkaline phosphatase exists in the periplasmic space of *E. coli* as a dimer of identical subunits each containing 429 amino acids (11). The four Cys residues are present as two intrachain disulfides. The monomers are synthesized as a preenzyme containing a Leu-rich signal peptide of 22 residues (7, 45, 56, 57). Processing occurs via a signal peptidase after secretion through the membrane (17). Recent data suggest that formation of active enzyme upon dimerization may be a complex process involving some modulator molecules (J. F. Chlebowski, personal communication).

A comparison of the amino acid sequences of the phosphorylated peptides isolated from the enzyme with the complete amino acid sequence showed that the phosphorylated residue was Ser102. Figure 1a shows the overall shape and polypeptide conformation found in the crystal structure of the dimer. Figure 1b shows a ribbon diagram of the secondary structure of the monomer.

* SUMMARY OF SUBSTRATE SPECIFICITY AND KINETICS OF ALKALINE PHOSPHATASE

Alkaline phosphatase is thought to be strictly a phosphomonoesterase, although one recent investigation found a low phosphodiesterase activity

MASS
SPEC?

444

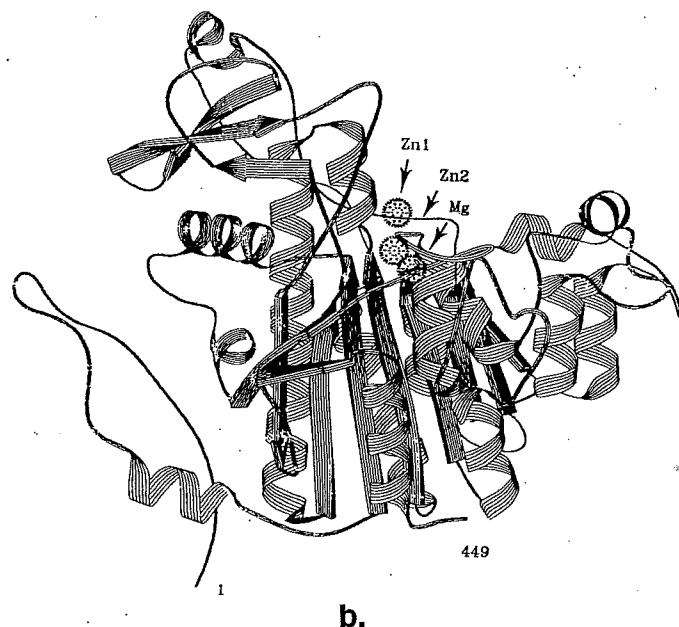
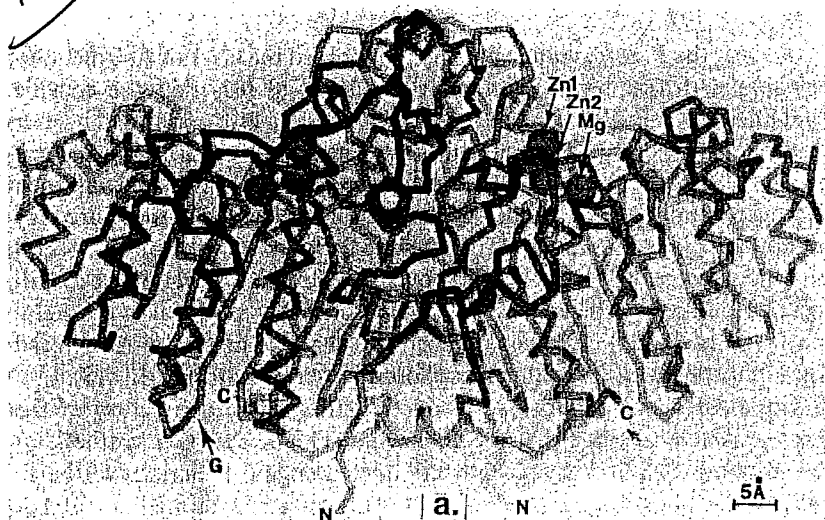
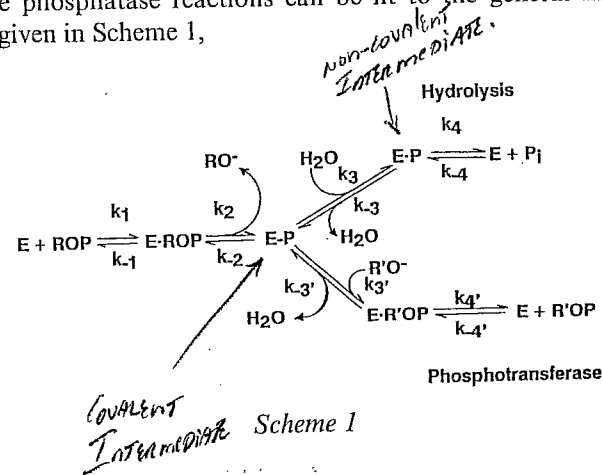


Figure 1 (a) Alpha-carbon trace of the dimer of *E. coli* alkaline phosphatase. The non-crystallographic two-fold axis is vertical and the maximum dimension of the dimer is horizontal. The three metal ions at each active center are shown as spheres and the two active sites of the dimer are 30 Å apart. (b) Ribbon drawing of the monomer of *E. coli* alkaline phosphatase. The three metal ions are shown as stippled spheres, Zn1, Zn2, and Mg as indicated. The center of the monomer consists of a 10-stranded β -sheet flanked by 15 helices of varying lengths. A second 3-stranded β -sheet and an α -helix form the top of the molecule in this view. Reprinted from Ref. 48.

TABLE I
Fig. 2.
*

(J. F. Chlebowski, personal communication). The enzyme hydrolyzes not only oxyphosphate monoesters (23, 29, 41, 63), but also a variety of O- (58, 59) and S-phosphorothioates (19), phosphoramidates (63), thiophosphate, and phosphate (3, 19, 65, 69); hydrolysis of the latter group is reflected by the catalysis of the exchange of ^{18}O from H_2^{18}O into inorganic phosphate (3, 65, 69) or the release of H_2S from thiophosphate (19). The enzyme has an alkaline pH maximum, and the rate follows an approximately sigmoid pH-rate profile with an apparent pK_a of ~ 7.5 (19, 34, 50, 63). Table 1 summarizes substrate structure, reaction products, and k_{cat} values. In the case of oxyphosphate monoesters, the k_{cat} is apparently independent of the R group, which can vary from a large protein molecule to a methyl group (63). This finding reflects the fact that either the dephosphorylation of E-P or the dissociation of the product, P_i , is the rate-controlling step depending on pH. A variety of NMR methods have demonstrated that the latter step is rate limiting at alkaline pH (38, 44). In hydrolysis of P_i (^{18}O exchange) or release of H_2S , however, the phosphorylation of Ser102 by the substrate appears to be so slow as to be rate controlling (9, 19, 63).

Alkaline phosphatase reactions can be fit to the general kinetic formulation given in Scheme 1,



which includes the covalent phosphoseryl intermediate. E-P, formed when Ser102 is phosphorylated, and the noncovalent complex, E·P, which is formed with the product, P_i . At pH 5.5 and below, the $\text{E-P} \rightleftharpoons \text{E} \cdot \text{P}$ equilibrium favors E·P such that P_i can phosphorylate Ser102 to form high equilibrium concentrations of E·P (for summary, see 63). Scheme 1 also includes the finding that solvent, H_2O , is not the only acceptor for the phosphate from E-P. Almost any alcohol will serve as an acceptor at pH values above 9 and acceptor concentrations near 1 M as shown by recent ^{31}P NMR assays (38). Traditionally, amino alcohols with the amino group

Table 1 Values of k_{cat} for phosphate monoesters hydrolyzed by alkaline phosphatase

Substrate (conditions)	k_{cat} , pH 8.0 (s^{-1})
ROPO ₃ ²⁻ (0.1 M Tris)	8.5 ^a
ROPO ₃ ²⁻ (1.0 M Tris)	13-45
ROPO ₃ ²⁻ (1.0 M Tris), Co(II)	≈2
RSPO ₃ ²⁻ (1.0 M Tris)	30
RNHPO ₃ ²⁻ (1.0 M Tris)	28
ROPSO ₂ ²⁻ (0.1 M Tris)	0.005
ROPSO ₂ ²⁻ (1.0 M Tris)	0.09
ROPSO ₂ ²⁻ (1.0 M Tris), Co(II)	0.17
HSPO ₃ ²⁻	0.26
HOPO ₃ ²⁻	0.15-0.2

^a When a single k_{cat} is given, it stands for a representative value for substrates that have been the subject of relatively few studies. If a range is given, it reflects a substrate for which a great many values of V_{max} are available in the literature.

on the carbon adjacent to that carrying the accepting OH, e.g. Tris and ethanolamine, have been used to demonstrate this phosphotransferase activity (63). These acceptors not only have enhanced acceptor activity, but show maximum transferase activity around pH 8 (63). The rate rapidly falls off at higher pH values, pH 8-11 (38). Analysis of the high-resolution crystal structure does not as yet suggest the reason for this special reactivity of amino alcohols. The mechanism of the phosphotransferase activity based on a variety of NMR evidence is postulated to involve the coordination of the alcoxide ion to one of the zinc ions at the active site instead of a water molecule (38).

Since the original isolation of a phosphorylated serine from alkaline phosphatase by Engström's laboratory (27, 28), kinetic analyses of the enzyme reaction have included steps for the formation and dephosphorylation of the serylphosphate. Rapid-flow kinetic methods applied to examine the initial phases of the hydrolysis of nitrophenyl phosphates by the enzyme revealed that the enzyme produced a relatively rapid burst of phenolate product followed by a steady-state rate at acid pH, but no burst was observed at alkaline pH, where the enzyme was maximally active. The acid burst was readily explained by the finding that dephosphorylation of E-P was very slow, $0.1 s^{-1}$, and rate limiting. The possible rate-limiting step at alkaline pH was less clear. The rate of phosphorylation of the serine hydroxyl at pH 5.5, calculated from the burst rate, ranged from 17 to $30 s^{-1}$ as assembled from numerous studies. In 1973, Bloch & Schlessinger

(8) demonstrated that the rapid-flow kinetics were badly distorted by phosphate that was bound to the native enzyme and carried along through most standard isolation procedures. When phosphate-free enzyme was employed for rapid-flow measurements, they observed instantaneous bursts of RO⁻ (within the 3-ms dead time of the instrument) at both pH 5.5 and 8.0. The readdition of phosphate abolished the burst at alkaline pH and slowed down the burst rate at acid pH. Thus, contaminating phosphate can abolish the burst at alkaline pH by the prior formation of E·P, but in general cannot completely abolish the burst at pH 5.5, because E-P is not 100% formed. Even more importantly, most stock enzymes were diluted from neutral pH where no E-P was present at the time of mixing. Thus, HOPO₄²⁻ simply competed with ROPO₄²⁻ binding at acid pH. Because phosphorylation from the monoester is so much more rapid than from phosphate, the rate of release of RO⁻ slowed during the transient phase, despite the fact that the ester still carried out most of the phosphorylation of the enzyme. An important fact emerging from these studies is that phosphorylation from ROPO₄²⁻, even at acid pH, is a much more rapid process than previously believed. Since the bursts at both pH 5.5 and pH 8.0 are instantaneous, k_2 , the phosphorylation rate in Scheme 1, must be at least $300 s^{-1}$ throughout the pH range from pH 5.5 to 8.0 and may be even faster.

The values of many of the kinetic and equilibrium constants describing the alkaline phosphatase reaction (Scheme 1) are plotted in Figure 2 as a function of pH. The pH-rate profile, expressed as k_{cat} , is presented as a sigmoid function corresponding to a single pK_a of 7.5 (Figure 2a). After collection of most of the published data on pH-rate profiles for the *E. coli* enzyme, this curve was chosen to represent k_{cat} (see 19, 50, 58, 65). Although not all pH-rate profiles fit the theoretical curve for a single ionization, the most extensive analyses of pH-rate profile data using Dixon plots ($\log V_{max}$ vs pH) show that the pH-rate profile can be adequately fit by a single pK_a (50). This finding suggests, but does not prove, that a single proton dissociation is involved. Under conditions usually employed for alkaline phosphatase assays, the pK_a for V_{max} is ~7.5; however, depending on whether neutral buffers, cationic buffers or added organic solvents are present, the apparent pK_a has been observed to vary from 6.58 to 7.55 (50). K_m values for phosphate monoesters remain constant as a function of pH until above pH 8, where an increase in the magnitude of K_m can be fit with an apparent pK_a near 9 (Figure 2b) (50). Thus, V_{max}/K_m plots are bell-shaped if high pH values are included. The increase in K_m at high pH may be connected with a phenomenon of phosphate dissociation at high pH observed using ³¹P NMR and discussed further below.

Direct measurements of k_3 , the rate for dephosphorylation of the phos-

Fig 2
pKa (Vmax) ~ 7.5
Km ↑ when pH > 8

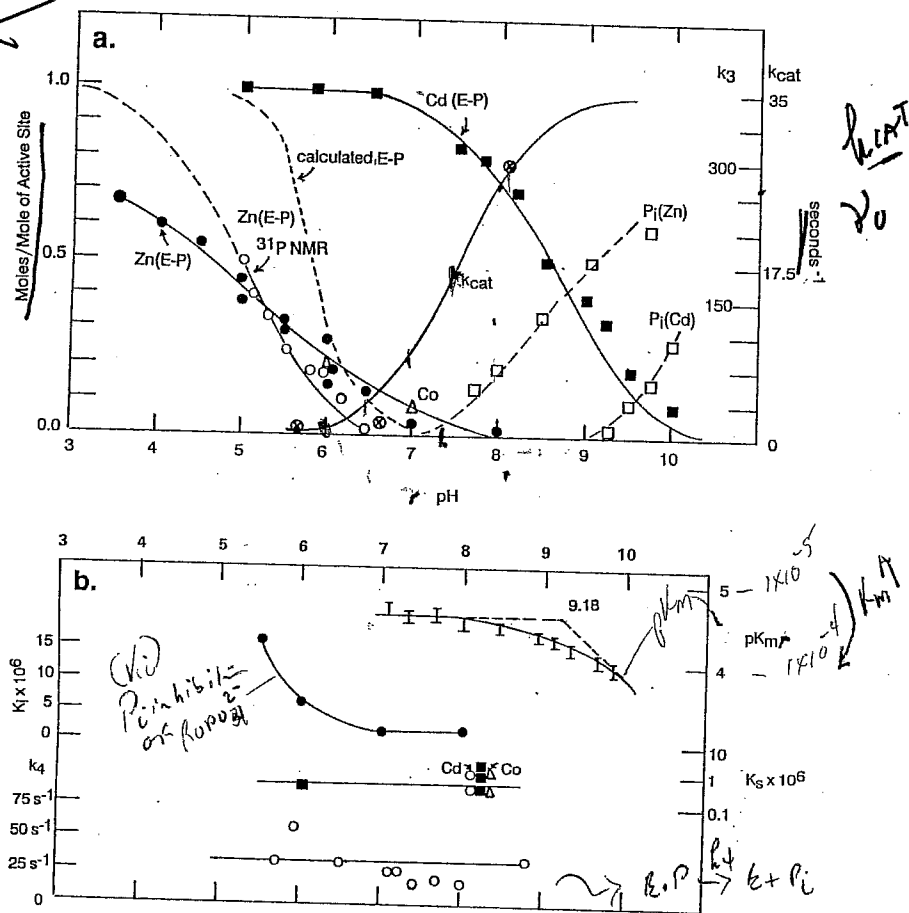
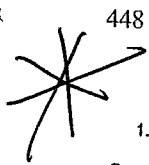


Figure 2 Summary of kinetic constants, equilibrium constants, and concentration of phosphoenzyme intermediates describing the interaction of phosphate monoesters and phosphate with *E. coli* alkaline phosphatase as functions of pH. (a) (Solid circle) Moles of E-³²P formed per mole of active site by the native zinc enzyme. (Open circle) E-P per mole of active site as determined using ³¹P NMR. (Dashed line) Expected moles of E-P formed per mole of active site calculated from kinetic constants (52). (Solid square) E-P formed by Cd₆AP per mole of active site as determined by labeling with H³²PO₄²⁻ and using ³¹P NMR. (Open triangle) E-³²P formed by CoAP. (Solid line) The central sigmoid curve labeled k_{cat} represents the pH-profile of k_{cat} (see text). (Circled X) k₃, value for the desphosphorylation rate of E-P determined as described in the text. (Open square) P_i (moles per mole of active site) dissociating from the Zn₄Mg₂⁻ and Cd₆ alkaline phosphatase; at acid pH, both enzymes bind 2 mol of phosphate per mole of dimer. (b) (I) K_m for hydrolysis of ROPO₄²⁻. (Solid circle) K_i for inhibition of ROPO₄²⁻ hydrolysis by phosphate. K_s represents equilibrium constants for ³²P binding to AP as determined by equilibrium dialysis for the Zn (solid square), Cd (open circle) and Co (open triangle) enzymes. (Open circle) k₄, dissociation rate of phosphate from E-P as determined using ³¹P NMR in version transfer.

phoseryl residue (E-P), are difficult to obtain. The relatively few values in the literature are those calculated in order to fit reaction profiles observed in rapid flow kinetics. Because $k_{-3}/k_3 = E\text{-P}/E\cdot P$, many reasonably accurate values of this ratio are available. Estimates of k_3 vs pH taken from kinetic analyses of the alkaline phosphatase reaction are plotted in Figure 2a. Because most rapid-flow kinetics studied prior to 1973 were distorted by the presence of contaminating inorganic phosphate bound to the enzyme (8), some modification of the estimates of the magnitude of k_3 are required, especially at alkaline pH. One can determine a lower limit for k_3 from the dead time of the stopped-flow instrument because an instantaneous burst of ~ 1 mol of RO⁻ per mole of active site is observed at alkaline pH for the phosphate-free enzyme and because this burst results from the slow, 35 s⁻¹, rate-limiting dissociation of E·P. Therefore, as noted above, k_3 must be ≥ 300 s⁻¹ at pH 8.0; the scale for k_3 in Figure 2a has been adjusted to reflect this.

The equilibrium concentration of E-P (1.0 represents maximum possible formation of phosphoserine) for the Zn, Co, and Cd enzymes has been plotted from data obtained by ³²P labeling of the enzyme by incubation with H³²PO₄²⁻ \rightleftharpoons H₂³²PO₄⁻, followed by manual quenching (3, 65). The curve marked "calculated" is the equilibrium concentration of E-P formed as a function of pH predicted by Wilson and his colleagues from the kinetic constants for the E-P \rightleftharpoons E·P \rightleftharpoons E + P_i reaction as assembled from the extensive kinetic data (52). These investigators suggested that the reason the predicted curve is steeper than the observed values obtained from several laboratories using ³²P labeling is the difficulty of quenching the enzyme rapidly enough to trap all the phosphoserine.

The E-P \rightleftharpoons E·P equilibrium vs pH also has been determined using ³¹P NMR to avoid perturbing the equilibrium by the method of detection. The ³¹P NMR of the enzyme-bound phosphate can quantitate these two intermediates from pH 10 to 5. Between pH 7 and 10, no detectable E-P is present at equilibrium. Between pH 7 and 5, the ratio of E-P/E·P rises along a sigmoid-curve and reaches a value of 1 at pH 5. Below pH 5, the zinc enzyme is unstable. Because the ratio is determined accurately by ³¹P NMR at close intervals over half the pH function, one can extrapolate a sigmoid function for the E-P/E·P with a midpoint at pH 5 as shown in Figure 2a. Values of k₄ for dissociation of P_i remain relatively constant from pH 5.7 to 8.8 as determined using ³¹P NMR inversion transfer (Figure 2b) (Table 2) (38). Values of the equilibrium constant for phosphate binding, K_s, as determined by equilibrium dialysis using H³²PO₄²⁻ are shown for pH 6 and pH 8.8, the latter for the Zn, Co, and Cd enzymes (3). For the Zn enzyme, K_i values for phosphate kinetically determined by Wilson's laboratory are shown for pH values of 5.5, 6.0, 7.0, and 8.0 (52).

Table 2 Dissociation rates of the product, inorganic phosphate, from the active site of alkaline phosphatase as a function of the metal ion composition of the enzyme^a

Enzyme	k_{off} (s^{-1})
Zn(II) ₄ AP (pH 8.8)	35
Zn(II) ₄ AP (pH 5.7)	33
Zn(II) ₄ AP + 1.0 M Cl ⁻ (pH 8.0)	60–260 ^b
[Zn(II) _A Mg(II) _B] ₂ AP (pH 8.0)	≈ 1
[Zn(II) _A Mg(II) _B] ₂ AP + 0.1 M Cl ⁻ (pH 9.0)	1.8
[Zn(II) _A Mg(II) _B] ₂ AP + 1 M Cl ⁻ (pH 9.0)	≈ 15
[Zn(II) _A Cd(II) _B] ₂ AP (pH 9.0)	≈ 2
Cd(II) ₆ AP (pH 9.0)	< 1
Cd(II) ₆ AP + 1 M Cl ⁻ (pH 9.0)	≈ 10

^a All samples were in 0.01 M Tris-acetate (38).

^b Too fast to measure directly by ³¹P NMR inversion transfer; limits given are based on the inversion transfer measurement at 162 MHz.

The value of k_3 , the dephosphorylation rate of E·P, falls rapidly from pH 8.0 ($\geq 300 \text{ s}^{-1}$) to pH 6.3 ($\sim 1.3 \text{ s}^{-1}$), over the same pH range in which k_{cat} falls by $\sim 90\%$ (Figure 2a). Thus, the pH-rate profile (from alkaline to acid pH) is coincident with a change in the rate-limiting step from phosphate dissociation to dephosphorylation of the phosphoserine. At pH 8, k_3 exceeds the rate of dissociation of the product phosphate, k_4 , by ~ 10 -fold. At pH 6.3, however, the relationship is reversed; k_4 is 26-fold faster than k_3 and is no longer rate limiting. On the other hand, k_3 is not yet as slow as k_{-3} , the rate of phosphorylation of Ser102 from E·P, and thus significant equilibrium concentrations of E·P are not observed at pH 6.3. At pH 5, k_3 has decreased further such that $k_3 = k_{-3}$ and $[\text{E} \cdot \text{P}] = [\text{E} \cdot \text{P}]$ at equilibrium (Figure 2a). Judging by ¹⁸O exchange experiments, both constants must be on the order of 0.1 s^{-1} . The possible identity of the $\text{AH} \rightleftharpoons \text{A}^- + \text{H}^+$ equilibria governing k_3 and the pH-rate profile are discussed in the section on structure and mechanism.

Phosphate is both a substrate and competitive inhibitor of the enzyme. Phosphate binding appears to be essentially pH independent between pH 5.5 and 8.0 if the values for K_i and K_s are taken as a guide (Figure 2b) (3, 52, 63). In support of this conclusion is the fact that the dissociation rate of inorganic phosphate from the enzyme, k_4 , is also pH independent from pH 5.5 to 8.8 (38). A pH independence of phosphate binding to alkaline phosphatase is surprising because two proton dissociations of phosphoric acid may fall in the pH range 5 to 10, $\text{H}_2\text{PO}_4^- \rightleftharpoons \text{HPO}_4^{2-} + \text{H}^+$ ($\text{pK}_a = 6.8$) and $\text{HPO}_4^{2-} \rightleftharpoons \text{PO}_4^{3-} + \text{H}^+$ (normal $\text{pK}_a \approx 12$). The latter could affect the

AP-phosphate equilibrium if E·P forces formation of the trianion as some reasoning suggests (see below). An enzyme active center, which excludes all but specific water molecules, may limit proton access from the bulk solvent as well. Even in the apophosphoryl enzyme, which is formed by removing Cd from the E·P form of the enzyme, the ³¹P chemical shift shows that the dianion form of the phosphoserine group is not titrated to become the monoanion until below pH 4.0 after the enzyme unfolds (34).

At variance with the kinetic constants that suggest that phosphate binding is pH independent is the observation, made using ³¹P NMR, that while Zn₄AP remains saturated with phosphate to pH 7.0, above pH 7.0 bound phosphate significantly decreases such that $[\text{E} \cdot \text{P}] = [\text{P}_i]$ at pH 10 (Figure 2a) when enzyme is 2 mM and phosphate 4 mM (33). The latter finding appears paradoxical, since the measurement of k_4 by NMR inversion transfer shows that the dissociation rate remains constant at $\sim 35 \text{ s}^{-1}$ under the same conditions and over the same pH range (Figure 2b). While one could postulate that the "on" constant for phosphate binding changes at high pH, this seems unlikely. If a water molecule on Zn_A becomes Zn-OH at alkaline pH, phosphate binding will compete with hydroxide binding to Zn_A. In support of this postulate is the observation that phosphate does not begin to dissociate from the cadmium enzyme until well above pH 9.0 (Figure 2a) (33). However, if both bound phosphates on the enzyme were competing equally with OH⁻, then k_4 should increase as it does in the case of Cl⁻ competition (Table 2). One possible explanation of this paradox is negative cooperativity of phosphate binding, i.e. phosphate at one active site is bound less tightly than at the other at pH values above 7.0. Then most of the remaining E·P will be at the tight binding site and the inversion transfer will be weighted in favor of this site.

Negative cooperativity has not been discussed thus far in this review. The phenomenon formed a significant part of earlier discussions of the alkaline phosphatase reaction because many early experiments measuring H³²PO₄²⁻ binding or burst magnitude showed that only a single bound phosphate per dimer or a single active site was phosphorylated. When sample-preparation techniques were changed such that samples with a full complement of metal ions were prepared, two E·P or two E·P complexes per dimer were easily formed under most conditions, especially at pH values below 7. Note that the Cd₆AP retains 1 mol of E·P per active site or 2 mol/dimer until the pH rises above 7.0 (Figure 2a). From pH 7 to 9, the sum of E·P + E·P also remains 2/dimer for the Cd₆ enzyme (32). Likewise, when enzymes uncontaminated with phosphate were employed in rapid-flow experiments, most burst stoichiometries approached 2/dimer (8).

Before we discard negative cooperativity in alkaline phosphatase as an

artifact, however, I must point out that in the alkaline pH range several sensitive NMR techniques can detect unequal binding constants for the two enzyme-bound phosphates. Detailed ^{31}P NMR titrations of the Zn_4AP and the Cd_6AP with P_i show that at pH 6 both enzymes titrate linearly the formation of 2 mol of enzyme-bound phosphate per mole of dimer. The Cd_6AP does the same at pH 8, but the Zn_4AP titrates the formation of only 1 mol of E·P under the NMR conditions employed (33). The same phenomenon is apparent when phosphate binding to the enzyme is evidenced by ^{35}Cl line broadening resulting from the binding of two $^{35}\text{Cl}^-$ ions to each Zn_A . At pH 6, the phosphate ions displace one chloride from each Zn_A site, i.e. half the Cl^- . In contrast, at pH 8 one phosphate displaces only one quarter of this Cl^- in a stoichiometric fashion; displacement of the other quarter requires up to six phosphates per dimer (37). Thus, inequivalent phosphate binding affinities may be involved in product release.

The rate-limiting phosphate product dissociation accounts for burst kinetics observed at alkaline pH by stopped-flow methods when a phosphate-free enzyme is employed (5, 20). Because the enzyme does not appear to recognize the R group of a phosphomonoester, researchers have often assumed that phosphate ester binding affinity was similar to that of phosphate. Indeed, the best measurement of K_m values have been $\sim 10^{-6}$ M for ROPO_3^{2-} , although they increase to almost 10^{-4} M for an O-phosphorothioate, ROPSO_2^- (19, 58). When an acceptor alcohol is present, the rate of the phosphotransferase activity is always additive to that of the initial phosphohydrolase as has been confirmed using accurate ^{31}P -NMR measurement techniques (38). Because the dissociation of P_i is rate limiting for the hydrolysis reaction under these conditions, the dissociation of the new product ester in the transferase reaction is clearly considerably more rapid than phosphate dissociation. K_m varies as a function of the metal ion species, Zn or Co, at the active center (19), but the K_i for phosphate is rather similar for the Zn, Co, and Cd enzymes [$(0.75 \pm 0.25) \times 10^{-6}$ M] (3). If the dissociation rate constant for ROPO_3^{2-} were $\sim 35 \text{ s}^{-1}$ as it is for phosphate, then K_m would not represent k_{-1}/k_1 , since the phosphorylation rate at pH 8 is at least 10^2 s^{-1} and probably even faster.

In comparing the kinetic pattern observed for phosphate esters as substrates and the information derived from using phosphate as substrate to form E·P, one should keep in mind that phosphorylation of the enzyme by HOPO_3^{2-} has become rate-limiting, as concluded from the fact that the ^{18}O exchange rate, 0.1 to 0.2 s^{-1} , is slower than the dephosphorylation of E·P over most of the pH range and is always slower than the dissociation of P_i . The ^{18}O exchange reaction is pH independent, evidence that the apparent pK_a reflected in the normal pH-rate profile is that of a group

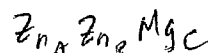
primarily affecting a step following formation of the phosphoseryl intermediate (see below). This pH independence, presumably controlled by a slow phosphorylation, is confirmed by the hydrolysis of thiophosphate, which releases H_2S (19). The rate of release of H_2S from thiophosphate is the same at pH 5.5 and 8.0 and is only slightly more rapid than the rate of ^{18}O exchange into phosphate catalyzed by the enzyme (Table 1).

The above background is useful in considerations of the nature of the transition state in the alkaline phosphatase mechanism and whether the reaction is primarily associative via the initial attack of the Ser-O^- on the phosphorous or whether the enzyme mechanism involves significant dissociative features via activation of the leaving group as in non-enzyme-catalyzed phosphomonoester hydrolysis (6, 49, 78). Recent investigations have probed this question and confirmed that k_{cat}/K_m values for a variety of substrates as functions of the pK_a of the leaving group show β values of ~ 0.1 rather than the value of ~ 1 expected for a dissociative reaction (51, 78). Although these newer findings and earlier, less rigorous kinetics have been interpreted to mean that the enzyme mechanism is purely nucleophilic in character, forming a five-coordinate intermediate, the high resolution crystal structure of E·P reveals interesting structural arrangements of metal and phosphate that bear on this view of the mechanism, as discussed in the next section of this perspective.

Using the phosphotransferase reaction to capture as a second chiral phosphate ester the phosphate from E·P initially formed by a chiral phosphomonoester containing ^{16}O , ^{17}O , and ^{18}O , Jones et al (46) demonstrated that the alkaline phosphatase reaction proceeds with retention of configuration around phosphorus. This result suggested that the reaction path consists of two in-line nucleophilic attacks; the first by the Ser-OH (or Ser-O $^-$) and the second by solvent H_2O (or ^-OH).

THE METALLOENZYME NATURE OF ALKALINE PHOSPHATASE

The original analytical data reporting that alkaline phosphatase was a Zn metalloenzyme showed two Zn ions per dimer (62). Subsequent determinations of the zinc content by the original laboratory and other investigators showed that with different preparation techniques the Zn:protein dimer ratio was generally 4 and under some circumstances could reach 6 (1, 10, 25, 60). Numerous studies contribute to these conclusions; it is now certain that a fully active native alkaline phosphatase contains four Zn and two Mg ions, the Zn occupying sites designated A and B, while Mg occupies sites designated as C. The A, B, and C sites were first unequivocally demonstrated using ^{113}Cd NMR. The $^{113}\text{Cd}_6$ enzyme shows three



NO

4 Zn / Dimer
2 Mg

of simultaneously following the phosphotransferase and hydrolysis reactions (38). Most phosphate monoesters, even those with relatively similar R groups, have sufficiently different ^{31}P chemical shifts to be distinguished. The separate signals for *p*-nitrophenylphosphate, P_i , and phospho-Tris are shown in Figure 8a illustrating a ^{31}P NMR spectrum of a standard assay mix (20 mM *p*-nitrophenylphosphate-1 M Tris) a few minutes after adding assay concentrations of alkaline phosphatase.

Figure 8b shows examples of the pH-dependencies of phosphotransferase reactions as followed by ^{31}P NMR, employing two rather different acceptors, Tris and glycerol. The data are presented as the ratio of new ester product to the hydrolysis product, phosphate, as a function of time, which is also the ratio of the rates of the two separate reactions,

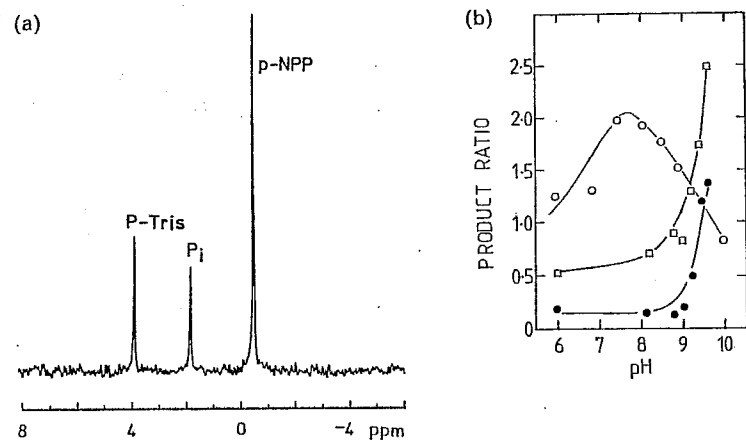


Figure 8 (a) ^{31}P NMR (80.9 MHz) spectra of substrate, *p*-nitrophenyl phosphate and products, inorganic phosphate, and O-Tris phosphate during hydrolysis and phosphotransfer as catalyzed by alkaline phosphatase. The composition at the start of reaction was 20 mM *p*-nitrophenyl phosphate in 1 M Tris or 3 M glycerol, pH 8, 293 K. To this was added alkaline phosphatase (5×10^{-8} M). The spectra were collected after about 50% hydrolysis and represent 80 scans. (b) pH Dependence of transferase and hydrolase products in the presence of 1 M Tris and 3 M glycerol. (Open circle) Ratio of initial rates of formation of Tris phosphate to inorganic phosphate; (open square) ratio of initial rates of formation of glycerol C1, C3, and C2 monophosphate to inorganic phosphate; (solid circle) ratio of initial rates of formation of glycerol C2 monophosphate to glycerol C1, C3 monophosphate. Note that at pH 9.5 the C2 transferase product exceeds the C1 + C3 product by the ratio 1.3:1.0. The reaction mixture in the case of glycerol contained initially 3 M glycerol in 50 mM Tris (the latter solely as buffer and not at high enough concentration to result in competition with 3 M glycerol). Enzyme (10^{-7} - 10^{-8} M) was used depending on pH. The substrate concentration was 20 mM. The figure is reproduced from Ref. 38.

phosphotransferase/phosphohydrolyase. The two curves for glycerol represent the formation of the equivalent C1 + C3 monophosphates and the C2 monophosphate. All three hydroxyl groups of glycerol are approximately equally phosphorylated by the enzyme. Tris is a much more effective acceptor in the neutral pH range than glycerol. The phosphotransferase reaction also increases in rate as the pH approaches the pK_a of the amino group, ~ 8 for Tris (63). This observation led to the suggestion that the neutral species of the amino alcohols were the most effective acceptors (63). The transferase activity of Tris, however, peaks at pH 8, falling rapidly to higher pH values (Figure 8b). At pH 9 and above, nonamino alcohols like glycerol, ethanol, and propanol are substantially more efficient acceptors than Tris (Figure 8b).

The rapid increase in the phosphate transfer to aliphatic alcohols above pH 9 is compatible with an arrangement in which the accepting alcohol is in the alcoxide form when bound at the active center and accepts the phosphoryl group from the seryl phosphate intermediate (38). If the oxygen of the acceptor coordinates Zn_A , as seems likely (38), then the apparent pK_a of the -C-OH will be lowered. An alcoxide has also been postulated to be the form of ethanol bound to alcohol dehydrogenase (82), another zinc enzyme in which an open coordination position on a zinc ion is the driving force for the formation of the alcoxide below its pK_a . At concentrations 0.5 M or greater, Tris and glycerol shift the ^{113}Cd resonance from the A site upfield by 14 and 6 ppm, respectively, at pH 9 (38). These ^{113}Cd chemical shift changes may represent the displacement of a water ligand by the alcoxide of the acceptor (38). Both the enhanced acceptor efficiency of the amino alcohols below the pK_a of the amino group and the rapid decline upon deprotonation of the amino group (Figure 8b) could result from the lowering of the pK_a of the $-\text{CH}_2\text{-OH}$ group caused by the adjacent $-\text{C-NH}_3^+$ group such that the alcoxide of the amino alcohols is formed more readily (has a lower pK_a) below the pK_a of the amino group than when the neutral form of the amino group is present.

SUMMARY OF THE MECHANISM OF ALKALINE PHOSPHATASE AS BASED ON SOLUTION DATA AND THE CRYSTAL STRUCTURE

Figure 9 shows the Michaelis complex of the dianion of a phosphate monoester bound to the active center of Ser102 along with the steps leading to the phosphorylation of Ser102 and its subsequent dephosphorylation. The probable structural relationships are taken from the crystal structure of the E·P complex of the native zinc enzyme (Figure 4b) and the E·P complex of the cadmium enzyme (Figure 6b). Zn_A coordinates the ester

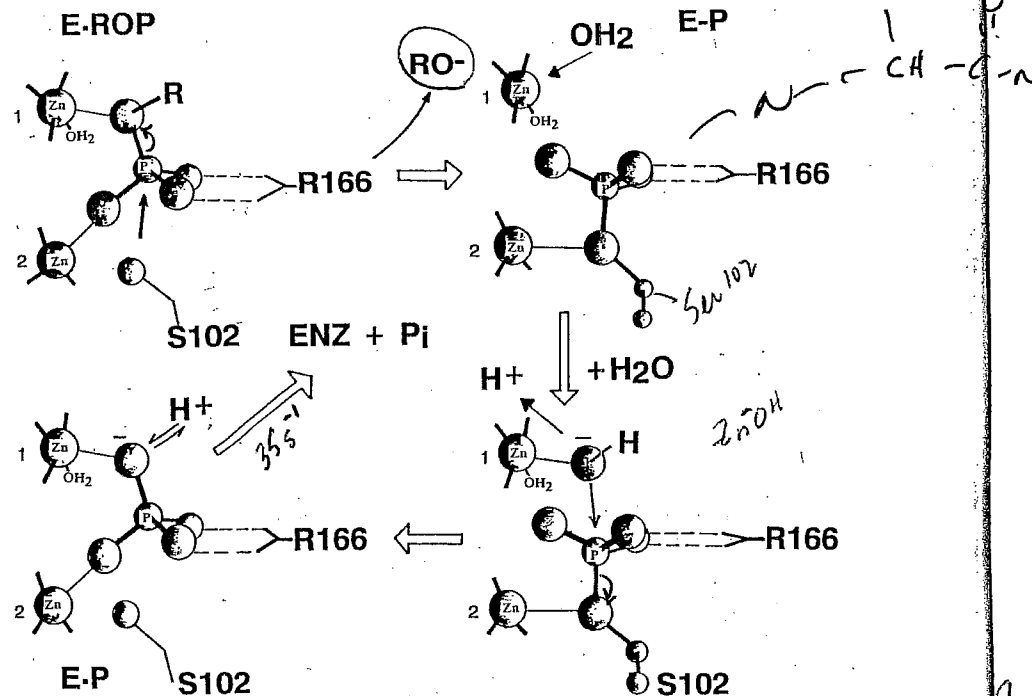


Figure 9 Major intermediates in the proposed mechanism of action of alkaline phosphatase. The dianion of a phosphate monoester, ROPO_3^{2-} , forms $\text{E}\cdot\text{ROP}$ in which the ester oxygen coordinates Zn_1 ; a second oxygen coordinates Zn_2 , forming a phosphate bridge between the Zn_1 and Zn_2 ; while the other two phosphate oxygens form hydrogen bonds (dashed lines) with the guanidino group of R166 . Ser102 is the nucleophile in the first half of the reaction and would occupy the position opposite to the leaving group, RO^- , in a five-coordinate intermediate. Upon formation of $\text{E}\cdot\text{P}$, the phosphate (as the dianion of a phosphoseryl residue) moves slightly into the cavity of the active center, but maintains a coordinate bond between Zn_2 and the ester oxygen as well as the two hydrogen bonds with R166 . A water molecule coordinates Zn_1 in the position occupied originally by the ester oxygen of the substrate. At alkaline pH, the water dissociates a proton to become Zn^-OH in position to be the nucleophile for the hydrolysis of the phosphoseryl ester. $\text{E}\cdot\text{P}$ forms as the phosphate moves away from the serine and as one of the phosphate oxygens again coordinates Zn_1 to reestablish a phosphate bridge. $\text{E}\cdot\text{P}$ is pictured as a phosphate trianion for the reasons discussed in the text. Dissociation of phosphate from $\text{E}\cdot\text{P}$ is the slowest, 35 s^{-1} , and therefore the rate-limiting, step.

oxygen, activating the leaving group. Zn_B , 3.9 Å away, coordinates a second phosphate oxygen, while the other two phosphate oxygens form hydrogen bonds with the guanidino group of Arg166 . The leaving group is pictured as the alcoxide, RO^- . Activation of this leaving group by the

A-site metal ion via a bond with the ester oxygen appears to be one of the functions of this ion in the first stage of the alkaline phosphatase reaction. The oxygen of Ser102 is in the other apical position to form the new ester bond with the phosphorous. Dissociation of RO^- and formation of the phosphoseryl intermediate is associated with movement of the phosphate farther into the cavity (Figure 6b). Hence, when the alcoxide leaves, its coordination site on Zn_A can be occupied by a water molecule that must dissociate a proton and become a Zn^-OH . The strongest evidence for this metal-induced proton dissociation is the large alkaline shift (3.7 pH units) in the pH dependence of the $\text{E}\cdot\text{P} \rightleftharpoons \text{E}\cdot\text{P}$ equilibrium when the much softer metal ion, Cd(II) , is substituted for Zn(II) . The Zn^-OH , placed in the apical position opposite to the seryl ester, occupies the place of the original leaving group and thus is ideally positioned to be the nucleophile in the second stage of the hydrolysis reaction (Figure 9).

The second stage of the reaction is nearly a mirror image of the first stage. Zn_B now activates the leaving group by forming a coordinate bond with the ester oxygen of the phosphoseryl residue (Figure 9). The hydroxyl coordinated to Zn_A attacks the phosphorous from the other apical position, and the transition state will decay into $\text{E}\cdot\text{P}$. The issue of whether the new phosphate oxygen remains negatively charged is discussed below, but the dissociation of phosphate anion in the $\text{E}\cdot\text{P}$ intermediate is remarkably slow, 35 s^{-1} .

As discussed in connection with the phosphotransferase reaction, why the dissociation of $\text{R}_2\text{OPO}_3^{2-}$ is more rapid than that of HOPO_3^{2-} if the latter is bound as the dianion is unclear. One possibility is that coordination of phosphate to both Zn ions as well as hydrogen bonding of the other two oxygens to the guanidino group of Arg166 forces the formation of the trianion, OPO_3^{3-} . On the other hand, the bound ROPO_3^{2-} can only be a dianion. Zn_A does seem to be capable of lowering the pK_a of bound water by several pH units as well as inducing the alcoxide in the phosphotransferase reaction. Thus, lowering the third pK_a of phosphate may not be so unexpected as it might at first appear. Such a postulate would provide an explanation as to why dissociation of phosphate from the active center is so much slower than that for the dianion of a phosphate ester. The higher negative-charge density would also explain why phosphorylation of Ser102 by both phosphate and thiophosphate is so slow compared to phosphorylation by any phosphate ester. The pK_a of the leaving group for thiophosphate, H_2S , is 6.9 compared to a pK_a of 15.7 for HOH , the leaving group in phosphorylation from phosphate. Yet in the presence of rate-controlling phosphorylation, the difference in the phosphorylation of Ser102 by these two agents is at most only twofold (Table 1), despite the large ΔpK_a between the leaving groups. If both substrates were bound as

trianions, poor leaving groups (probably requiring protonation first) and high charge density around the phosphorous could account for the very slow phosphorylation step as well as slow dissociation of the noncovalently bound species.

In the case of most enzyme-catalyzed phosphorylation or phosphotransferase reactions, investigators have tended to assume that such biological reactions were nucleophilic and associative and formed classic five-coordinate intermediates, the leaving group departing from the opposite apical position. This assumption was made despite the fact that in model systems most phosphate mono- and diester hydrolyses apparently proceed by a dissociative mechanism with the transient production of the highly electrophilic metaphosphate, $[\text{PO}_3^-]$ (6, 49, 78). Only phosphate triester hydrolysis follows a nucleophilic path in model systems (6, 49, 78). Enzymes could presumably make the nucleophilic path more favorable by creating protein-binding sites that successfully reduced the negative charge around phosphate, a significant inhibitory factor in mono- and diester hydrolysis in model systems. Determination of the predicted chirality changes around phosphate during enzyme-catalyzed phosphate incorporations, i.e. inversion if no covalent enzyme intermediate was formed and retention if a covalent enzyme intermediate was formed as in alkaline phosphatase, tended to solidify the nucleophilic point of view. However, the finding that the Zn ions activate the leaving group in both the initial phosphorylation of the active-center serine and its dephosphorylation suggests that there may be significant dissociative character to both reactions. While the enzyme might hold a metaphosphate rigid enough to prevent scrambling of chirality, the evidence that the phosphate oxygens exchange positions relatively rapidly in the Co(II) enzyme does not favor the existence of free PO_3^- at the active site. Whether a classic five-coordinate intermediate is a true transition state in the alkaline phosphatase reaction remains an open question.

20 SITE-DIRECTED MUTANTS OF *E. COLI* ALKALINE PHOSPHATASE

Cloning of the *phoA* gene has allowed researchers to employ site-directed mutagenesis to change several of the amino acid side chains at the active center of alkaline phosphatase. The results of mutations at Ser102 and Arg166 have been most informative relative to mechanism, while mutations of several surrounding residues have revealed subtle influences on the rate. The results of these mutations are summarized below.

Ser102 → *Cys102*, *Ala102*, *Leu102*

The Ser102 → Cys102 mutant shows between 30 and 90% of normal activity against *p*-nitrophenyl phosphate and 2,4-dinitrophenyl phosphate depending on conditions. The range of turnover values results both from the fact that the phosphotransferase/phosphohydrolase ratio is increased and that k_{cat} depends on the nature of the leaving group. The Cys102 enzyme has a k_{cat} of 4.6 s^{-1} with 4-nitrophenyl phosphate and a k_{cat} of 15 s^{-1} with 2,4-dinitrophenyl phosphate under conditions where k_{cat} for the wild-type enzyme is 18 s^{-1} (39). In addition, the pH profile of the Cys102 enzyme shows no clearly apparent pK_a of activity. Lastly, a covalent S-phosphorothioate cannot be isolated from the enzyme by quenching at low pH (39). Most of the above findings on the Cys102 mutant can be explained if the rate-limiting step has changed to phosphorylation throughout the pH range. Throughout the pH range, phosphorylation of the native enzyme by ROPO_4^{2-} occurs at the rate of 10^2 to 10^3 s^{-1} ; thus, the phosphorylation rate can fall by 10- or even 100-fold without significantly lowering k_{cat} . These findings also suggest that dephosphorylation of the S-phosphorothioate formed with Cys102 is occurring more rapidly than for the normal covalent intermediate. A detailed kinetic study is required to sort out the rate constants of the Cys102 mutant. Phosphotransfer from a ^{16}O -, ^{17}O -, and ^{18}O -labeled phosphate ester to an acceptor catalyzed by the Cys102 mutant revealed retention of configuration around the phosphorous, proving that the reaction pathway has not been substantially changed (12).

The Ser102 → Ala102 or Leu102 mutants are not completely devoid of activity. The k_{cat} values are reported to be $\sim 1/1000$ and $\sim 1/500$ of those for the wild-type enzyme (14). K_m values for ROPO_4^{2-} and K_i values for P_i are reported to be normal as is the pH-rate profile. Because residue 102 is not directly involved in the structure of E·P, the lack of alteration in substrate and phosphate binding is not surprising. Since Zn_A carries two coordinated H_2O molecules, as shown using NMR relaxation methods (37, 64), a water remaining on Zn_A may be in a position to directly attack the ester of E·ROP at a low rate. An alcoxide, R_2O^- , could do the same and account for the detection of some phospho-Tris formed by these mutants (14).

Arg166 → *Lys166*, *Glu166*, *Ser166*, *Ala166*

All four mutations of Arg166 result in enzymes that remain active but demonstrate an increase in K_m and a decrease in phosphate affinity (13, 15). Although a decrease in phosphate binding affinity might increase the